

Robust functionalization of amorphous cadmium sulfide films using z-lift amplitude modulated atomic force microscopy-assisted electrostatic nanolithography

Ivan Dolog, Robert R. Mallik, and Sergei F. Lyuksyutov^{a)}

Department of Physics, The University of Akron, Akron, Ohio 44325

(Received 15 February 2007; accepted 1 May 2007; published online 23 May 2007)

A robust technique, based on vertical (*z*-lift) manipulation of a negatively biased oscillating atomic force microscope cantilever, is developed which creates raised columnar nanostructures with high aspect ratios (up to 40 nm high/150 nm wide) on amorphous CdS thin films. The nanostructures' height (8–40 nm) is proportional to *z*-lift of the tip and correlates with CdS film thickness. An in-house modified electric force microscopy is used to record the associated surface charge distribution which is found to be opposite to that of the tip. © 2007 American Institute of Physics. [DOI: 10.1063/1.2742910]

CdS has been widely used in photovoltaic device applications for several decades. Recently, its importance as a component layer in the fabrication of tandem junction thin film¹ and annealed polycrystalline thin-film solar cells² has been recognized. It has also been incorporated in an oxygenated form (*a*-CdS:O) in polycrystalline CdTe based thin-film solar cells.³ The electronic transport properties,^{4–8} grain size distribution, and stoichiometry⁹ of polycrystalline CdS films have been studied extensively for some time. In this letter we fabricate ultrathin CdS films (~10–100 nm) by radio frequency (rf) sputtering and then employ a biased oscillating atomic force microscope (AFM) tip to create raised columnar nanostructures on the films. These nanostructures increase the effective surface area of the films and therefore may play a significant role in improving the efficiency of certain photovoltaic devices.

The present CdS films were deposited onto 100 nm thick Au–Pd sputter-coated silicon wafer substrates. The procedure has been described previously¹⁰ so only a brief description is given here. The films were rf sputtered in a background of argon at a pressure of ~50 mTorr using a high purity (99.999%) CdS target supplied by Kurt J. Lesker Co. A very low deposition rate (~0.01–0.02 nm s⁻¹) was employed to ensure smooth and uniform films as was confirmed by subsequent AFM imaging. Film thicknesses were determined *in situ* using a quartz crystal microbalance and ranged from 30 to 500 nm.

A patterning technique was used in this study to produce robust geometric functionalization of the films. The technique presents a unique combination of two techniques exploited previously, namely, amplitude modulated atomic force microscopy-assisted electrostatic nanolithography¹¹ (AFMEN) and *z*-lift AFMEN.¹² Both of these techniques were conceptually developed from AFMEN,¹³ a technique which generates features by mass transport of dielectric polymer macromolecules in the presence of a strong nonuniform electric field. These techniques^{11–13} have been shown to be effective for sacrificial surface reshaping of a wide range of thermoplastics and rigid rod polymers but have never been combined before the present work.

A Veeco Metrology Digital Instruments 3100 Dimensions AFM employing a Nanoscope IV controller was used in this study. A noncontact, highly conductive Micromash NSC12 ultrasharp cantilever, 90 μm long and 35 μm wide (force constant of 5 N m⁻¹), was mounted on an in-house modified tip holder isolated from the rest of electric circuits by a piece of insulating material. A piezoelement embedded in the tip-holder resonates typically at 2.5 V amplitude with the frequency of 240–315 kHz. C++, combined with a Digital Instruments nanolithography package, was used to manipulate the AFM tip through the following steps. First, the tip was brought towards the surface to a distance where the vibration amplitude (varied between 0.5 and 3.0 V) was suppressed by three orders of magnitude. An oscilloscope was used to monitor the tip's vertical deflection signal. The tip-surface separation for this event was selected as the reference point. Second, the tip, while oscillating, was raised to point A varied between 10 and 50 nm. Third, a bias voltage in the range of -10 to -40 V was applied to the tip which was slowly retracted to point B varied between 150 and 400 nm. The retraction speed varied from 50 to 200 nm s⁻¹ which allowed for a total exposure time of 0.5–2 s. The fourth step was lateral displacement of the tip at distance varied between 300 and 500 nm and back to the reference point. The cycle was then repeated to create more nanostructures. Schematically, this simple protocol named *z*-lift amplitude modulated (ZAM) (AFMEN) is presented in Fig. 1.

An in-house modified electric force microscopy (EFM) was used to monitor the electric charge distribution and its sign at the sample surface (see Fig. 2). The principles of EFM and its applications are described elsewhere.¹⁴ In our system a sweep function generator was used to apply a 25–30 kHz sinusoidal modulation reference signal with an amplitude of 4–5 V rms the AFM tip, and a digital lock-in amplifier was employed to recover the tip's vertical deflection. It is assumed that the associated electrostatic force due to the modulation signal has a negligible effect on the mechanical oscillations of the tip at 250–300 kHz.

The patterned nanostructures were imaged and their topography and electric charge distribution at the surface were recorded over a period of several seconds after the ZAM protocol was completed. The results are presented in Fig. 3. A comparison of the patterned features with corresponding

^{a)} Author to whom correspondence should be addressed; electronic mail: sfl@physics.uakron.edu

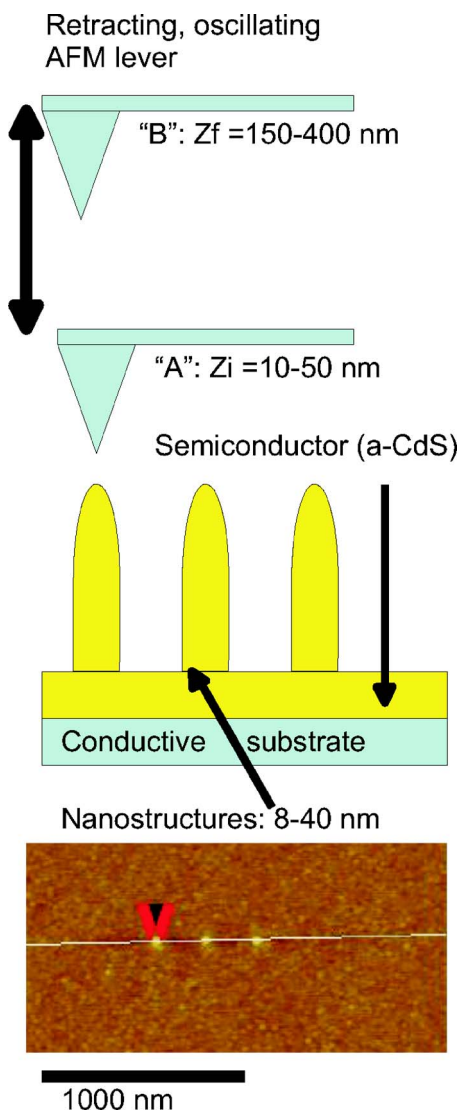


FIG. 1. (Color online) Schematic representation of the four-step ZAM protocol: First, a weakly biased AFM tip is brought towards the surface of the *a*-CdS film (whose thickness was in the range of 30–500 nm). Second, the tip is held at reference point A. Third, the AFM cantilever, oscillating at 240–330 kHz, is slowly retracted from point A to point B while simultaneously applying a bias voltage of –10 to –40 V; this step forms the nanostructures, 8–40 nm high and 50–150 nm wide, on the *a*-CdS surface. Bottom: Three dots formed using an exposure time of 2 s; the AFM tip was *z* lifted from 50 to 250 nm and the tip bias was –30 V.

EFM images from the same location indicates that the charge deposited on the CdS surface remains there for 5–10 min before it finally drains via the conductive substrate. However, AFM imaging of the nanostructures 7 days later showed no structural changes. EFM measurements indicated that the sign of the charge at the CdS surface was positive, i.e., opposite to that of the negatively biased AFM tip. It is well known that a weakly biased AFM tip forms a tiny water bridge under 20%–40% ambient humidity.¹⁵ Electric breakdown in water occurs in the presence of an electric field whose magnitude approaches 10^9 – 10^{10} V m⁻¹, which is the case for the present 10–20 V biased AFM tip separated from the surface by a distance of 0.5–2 nm. It has been reported recently¹⁶ that electric breakdown inside the water bridge initiates field-induced water ionization producing free carriers (electrons) as follows: $\text{H}_2\text{O}=\text{H}^++\text{OH}^-+e^-$. From the previous work, it is suspected that the abundance of electrons

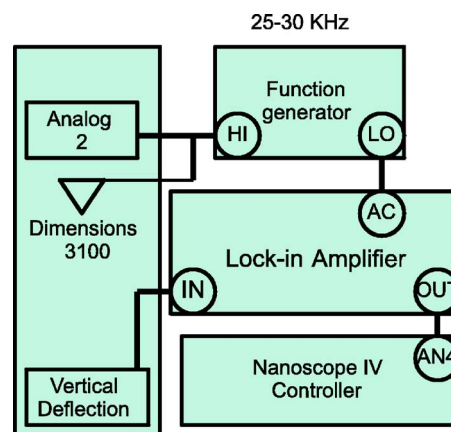


FIG. 2. (Color online) Block diagram of the electric force microscopy (EFM) technique. To reduce unwanted noise, an ac modulation signal (25–30 kHz, 4–5 V rms) is applied to the tip and the vertical deflection response signal (which contains information of surface electric potential) is recovered using a lock-in amplifier. The image is collected 30 s after the ZAM protocol is completed.

generated *inside* the water bridge is responsible for an anomalous electric current of 100–500 μA in magnitude observed on the surface of *n*-type Si, which has similar physical properties to CdS. Electric current studies suggest that elec-

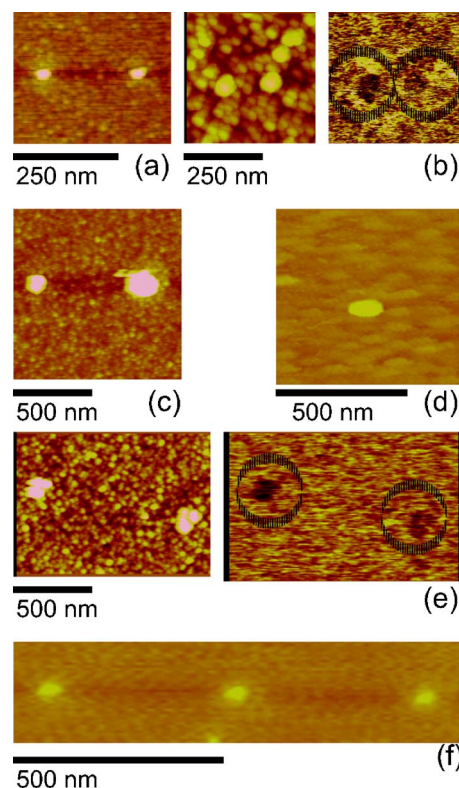


FIG. 3. (Color online) Examples of geometric functionalization of the *a*-CdS surface. (a) 30 nm (8 nm high dots), (b) 50 nm (22–25 nm high dots), (c) 100 nm (10–16 nm high dots), (d) 200 nm (40 nm high dots), and (e) 500 nm (35 nm high dots) films. The tip is retracted from the surface to a distance in the range of 50–250 nm; the tip bias is varied between –20 and –40 V. The height of the features increases from 8 to 40 nm, which appears to correlate with film thickness. EFM data suggest that positive electric charge is deposited on the surface (in the darker colored regions as shown) and dissipates 5–10 min later. However, all the physically patterned features remain intact for 7 days. (e) Example of silicon surface oxidation using the ZAM protocol (the tip is retracted from 50 to 250 nm and a negative bias of –15 V was applied): the height of the features was less than 3 nm.

tric breakdown in water is common and takes place in a variety of the systems involving high magnitude electric field and dielectric, or in semiconductor substrates and we anticipate this to be the case in the present CdS work.

The large dc electric field due to the biased AFM tip in proximity to the grounded CdS film may exceed 10^8 – 10^9 V m⁻¹ because of local structural variations of the tip and CdS surface; this field is sufficient to break Cd–S bonds and trigger ionized mass transport through the CdS films. However, electrochemical reactions at the CdS/water interface which may also produce Cd ions cannot be ruled out. For example, it has been proposed that photocorrosion of CdS occurs in the presence of dissolved oxygen in aqueous solution.^{17,18} In this photocorrosion process light is essentially an initiator which generates electron-hole pairs in the CdS films. After a series of reactions involving the CdS film, holes, and oxygen in the aqueous solution, the net result is that SO₄²⁻ and Cd²⁺ ions are the main photoproducts. In the present work we propose that the large electric field close to the biased AFM tip provides the energy required to create the electron-hole pairs in the initiation step. Then, once Cd ions have been created, oxidation mechanisms and/or mass transport of the Cd ions are possible causing deposition of oxide products and/or Cd ions at the CdS surface creating the observed nanostructures. This suggests transport of material vertically from below the nanostructures towards the surface along electric field lines. Clearly, further work is required to determine the exact nature of the mechanisms leading to nanostructure formation. A useful starting point would be the investigation of the following observations in support of a mass transport mechanism: (a) The height of the nanostructures (8–40 nm) patterned on CdS is much greater than that of structures patterned on silicon due to the surface scanning oxidation. ZAM protocol has been used to pattern nanostructures on crystalline Si(110) surfaces and the results indicate that their height does not exceed 3 nm. (b) The height of the structures on CdS appears to correlate with film thickness; we have observed 8 nm structures for a 30 nm film, 22–25 nm for a 50 nm film, 10–16 nm for 100 nm films, 40 nm for a 200 nm film, and 35 nm for 500 nm films. Future work to confirm this correlation would support the hypothesis that the material is displaced vertically. (c) The structures on CdS remain the same for a substantial period of time; if the sole mechanism for nanostructure formation were oxidation, the structures would be expected to change over time. This lends further support to our suggestion that a combination of processes is responsible for their formation.

In summary, we have developed a patterning technique, ZAM, which creates raised columnar nanostructures of 150 nm wide to 40 nm high on amorphous CdS films. Although sequential in nature, ZAM protocol allows robust geometric surface functionalization. It is anticipated that ZAM can be implemented for biological applications, precise surface modification, where large area functionalization is not required, and for photovoltaic applications in other semiconductors (possibly organic). Based on the height of the structures and their stability over time, it is suspected that a plausible physical explanation for the formation of these nanostructures is related to a combination of oxidation and ionized mass transport along the lines of very strong nonuniform electric field although further investigations are required to elicit the exact nature of these mechanisms.

The authors greatly acknowledge continuing support through AFOSR Grant No. F49620-02-1-428 in the frames of STW-21 Polymer Photonics Center.

- ¹A. D. Compaan, A. Gupta, S. Lee, S. Wang, and J. Drayton, *Sol. Energy* **77**, 815 (2004).
- ²C. C. Ferekides, R. Mamazza, U. Balasubramanian, and D. L. Morel, *Thin Solid Films* **480-481**, 471 (2005).
- ³X. Wu, Y. Yan, R. G. Dhere, Y. Zhang, J. Zhou, C. Perkins, and B. To, *Phys. Status Solidi C* **1**, 1062 (2004).
- ⁴R. G. Mankarious, *Solid-State Electron.* **7**, 702 (1964).
- ⁵L. L. Kasmerski, W. B. Berry, and C. W. Allen, *J. Appl. Phys.* **43**, 3515 (1972).
- ⁶C. Wu and R. H. Bube, *J. Appl. Phys.* **45**, 648 (1974).
- ⁷J. W. Orton, B. J. Goldsmith, J. A. Chapman, and M. J. Powell, *J. Appl. Phys.* **53**, 1602 (1982).
- ⁸I. Martil, G. Gonzalez-Diaz, and F. Sanchez-Quesada, *J. Vac. Sci. Technol. A* **2**, 1491 (1984).
- ⁹C. T. Tsai, D. S. Chuu, G. L. Chen, and S. L. Yang, *J. Appl. Phys.* **79**, 9105 (1996).
- ¹⁰I. Dolog, R. R. Mallik, A. Mozynski, and J. Hu, *Surf. Sci.* **600**, 2972 (2006).
- ¹¹S. F. Lyuksyutov, P. B. Paramonov, S. Juhl, and R. A. Vaia, *Appl. Phys. Lett.* **83**, 4405 (2003).
- ¹²S. Juhl, D. Phillips, R. A. Vaia, S. F. Lyuksyutov, and P. B. Paramonov, *Appl. Phys. Lett.* **85**, 3836 (2004).
- ¹³S. F. Lyuksyutov, R. A. Vaia, P. B. Paramonov, S. Juhl, L. Waterhouse, R. M. Ralich, G. Sigalov, and E. Sancaktar, *Nat. Mater.* **2**, 468 (2003).
- ¹⁴P. Girard, *Nanotechnology* **12**, 485 (2001).
- ¹⁵H. Bloess, G. Staikov, and J. Schultze, *Electrochim. Acta* **47**, 335 (2001).
- ¹⁶S. F. Lyuksyutov, P. B. Paramonov, I. Dolog, and R. M. Ralich, *Nanotechnology* **14**, 716 (2003).
- ¹⁷D. Meissner, R. Memming, and B. Kastening, *J. Phys. Chem.* **92**, 3476 (1988).
- ¹⁸D. Meissner, R. Memming, S. Li, S. Jesodharam, and M. Gratzel, *Ber. Bunsenges. Phys. Chem.* **89**, 301 (1985).